Applied Catalysis, 45 (1988) 281-290
Elsevier Science Publishers B.V., Amsterdam — Printed in The Netherlands

Studies on the Promotion of Nickel–Alumina Coprecipitated Catalysts

III. Cerium Oxide

H.G.J. LANSINK ROTGERINK, J.C. SLAA, J.G. VAN OMMEN and J.R.H. ROSS*

University of Twente, Faculty of Chemical Technology. P.O. Box 217, 7500 AE Enschede (The Netherlands)

(Received 5 April 1988, revised manuscript received 8 August 1988)

ABSTRACT

Three series of cerium-promoted nickel–alumina catalysts with different nickel-to-aluminium ratios each containing different amounts of cerium have been prepared and characterized. The calcination and reduction behaviour were found not to be altered by the presence of cerium. Part of the promoter was found to separate during the precipitation process as poorly crystalline CeO_2, the amount of which was largely determined by the drying temperature. This phase separation process was accompanied by a partial change in the valence state of the cerium. The effect of cerium on the nickel particle sizes was very small. Cerium enhances the activity of coprecipitated nickel–alumina catalysts in the carbon monoxide methanation reaction. This enhancement is accompanied by an increased apparent activation energy. Cerium- and lanthanum-promoted materials are compared with one another and it is concluded that although both promoters behave differently in determining the catalyst structure, their behaviour in the carbon monoxide methanation reaction is very similar and the specific activities of both types of material are nearly equal.

INTRODUCTION

In the last few years much research has been done on the promoting effects in $CO + H_2$ reactions of several oxides on certain metal catalysts. One group of such oxides is that of the lanthanides and actinides. These may be present as promoter (i.e. added to a supported metal), as support (to which the metal was added) or as a component in intermetallic compounds. In the last case, the lanthanide metal is transformed into its oxide form under reaction conditions.

In the previous paper in this series, we reported on the effects of lanthanum on the properties of coprecipitated nickel–alumina catalysts [1]. For a short review of the relevant literature, we refer to that publication. It was found that lanthanum influences the adsorption processes of both carbon monoxide and hydrogen, and further that it enhances the methanation activity by a factor of

0166-9834/88/$03.50

up to three. The apparent activation energy is also increased. The results showed that when lanthanum is added during the coprecipitation stage, this leads to a meta-stable structure in which the lanthanum ion is built into a mixed nickel–aluminium precursor. Furthermore, it was shown that the lanthanum of this nickel–aluminium–lanthanum precursor separates when it is subjected to hydrothermal treatment. Once this phase separation has taken place, the promoting effect of lanthanum on the catalytic activity has disappeared. This indicates that some sort of interaction between the lanthanum and the nickel must be present in order for the lanthanum oxide to give rise to a promoting effect. This interaction must be present throughout the whole preparation process of coprecipitation, washing, drying, calcination, reduction and passivation.

In this paper, we report on the effect of cerium on the catalytic behaviour of coprecipitated nickel–alumina catalysts. Three series of materials with different nickel-to-aluminium ratios, each having different amounts of cerium, were prepared and characterized. It is shown that the process used to dry the precursors plays a role in determining the structure of the catalysts. Furthermore, the effect of cerium on the nickel particle sizes was investigated. Specific activities are also reported and the cerium-promoted materials are compared with the equivalent lanthanum-promoted samples.

EXPERIMENTAL

Preparation

The preparation of the catalysts was carried out in nearly the same way as for the lanthanum-promoted nickel–alumina materials; the differences were that the precipitation solution contained $Ce(NO_3)_3 \cdot 6H_2O$, that the total metal concentration was 0.9 mol/dm^3 (instead of 0.5 as in the case of lanthanum-promoted materials), and that the precipitating agent was sodium carbonate (instead of potassium carbonate). For a full description of the precipitation process, we refer to the previous paper [1]. Each of the three series of cerium-promoted coprecipitates were made with different ratios of nickel to aluminium: *series C*: molar ratio Ni/Al = 2.5; *series D*: molar ratio Ni/Al = 3.0; *series E*: molar ratio Ni/Al = 9.0.

The samples from the C-series will hereafter be denoted as C-X, X being the mol percentage of cerium defined by: $X = (\text{mol Ce}/(\text{mol Ni} + \text{Al} + \text{Ce})) \cdot 100\%$ and those of the D- and E-series will be denoted as D-X and E-X respectively in a similar way.

The precipitation process took 30 min and no ageing was applied. The freshly precipitated samples were washed thoroughly with 1 dm^3 of deionised water (80 °C) and were then dried overnight at 70 or 110 °C in air. This was followed by a second washing and drying cycle; the second washing step was applied to

lower the sodium content as much as possible because all the alkali metals have a detrimental effect on the catalytic activity [2].

Calcination and reduction were carried out in a tube furnace. The samples were calcined in a stream of nitrogen at 350°C, after an initial increase of the temperature at a rate of 2°C/min. Reduction took place in a stream of 50% hydrogen in nitrogen at 600°C (series C and D) or at 400°C (series E), also after an initial temperature increase of 2°C/min. After reduction, the samples were passivated in a stream of 0.5% oxygen in nitrogen for 16 h. The same procedures were used earlier for the lanthanum promoted samples [1].

All chemicals used were pro-analysis quality and the gases were 99.999% pure.

Characterization

Chemical analyses were performed by atomic absorption spectroscopy (AAS) and X-ray fluorescence (XRF) in order to determine the contents of sodium and cerium respectively. The processes of calcination and reduction were followed by thermogravimetrical analysis (DTG-TGA), using the same gases as those used in the tube furnace.

Phase analysis and particle size measurements

Phase analysis measurements were carried out using X-ray powder diffraction (XRD, Philips PW1370, Ni-filtered Cu $K\alpha$ radiation). The samples were characterized at different stages of the preparation process: as the coprecipitate, as the calcined material and as the reduced and passivated phase.

The particle sizes of the passivated samples were calculated according to the procedure given in the previous article [1,3].

Activity measurements

Activity measurements were carried out using differential scanning calorimetry (DSC), following the same procedure as described earlier [1]. The H_2/CO ratio used was equal to 3.0.

RESULTS AND DISCUSSION

The precipitate

XRD-diagrams are given in Fig. 1 for several samples of the C-series (Ni/Al=2.5). The sample which contained no cerium (C-0), showed the diffraction pattern characteristic of takovite, in agreement with the results obtained earlier [4]. An extra phase was present in C-1.5; the diffraction peaks of the

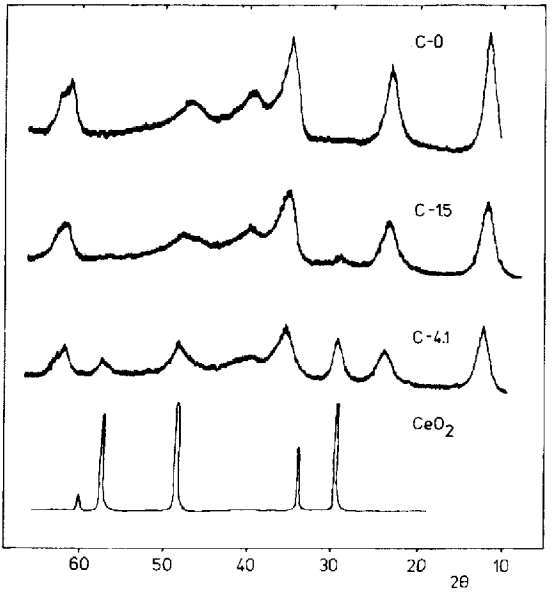

Fig. 1. XRD diagrams for samples of the C-series (Ni/Al = 2.5) and for CeO_2 (Cu $K\alpha$ radiation).

new phase became stronger with increasing amounts of cerium in the other members of the series, while those of the takovite phase decreased in intensity. The peaks of this new phase can be ascribed to poorly crystalline CeO_2, as is clear from Fig. 1, where the pattern for crystalline CeO_2 is also given. Whether or not all cerium in the samples C-1.5 and C-4.1 is present in this phase is not clear: it is possible that a small amount is taken up in the takovite compound although no evidence for this can be found from the XRD results. It appears that some or all of the Ce^{3+} of the precipitation solution is oxidized to Ce^{4+} and that phase separation of this phase occurs either during the precipitation or during the drying procedure. These results contrast with those of the lanthanum system [1]. In the lanthanum-promoted samples which had not been aged, phase separation occurred only at ≥ 5 mol-% lanthanum and this resulted in the formation of $La_2O(CO_3)_2 \cdot xH_2O$ with a high degree of crystallinity. At lower percentages, the lanthanum was built into the takovite structure.

The samples of the D-series behaved similarly to those of the C-series, phase separation already occurring at very small amounts of cerium. The samples of the E-series were more amorphous than those of the two other series and no extra CeO_2 phase was observed at cerium concentrations up to 2.7 mol-%; sample E-4.3, however, contained this phase.

The effect of the drying procedure can be seen in Fig. 2 which shows X-ray diffractograms of three samples of C-3.0 dried under different conditions: at 110 °C in air or at 70 °C in air or nitrogen. It is clear that the amount of CeO_2 which separates is determined largely by the drying temperature. The largest

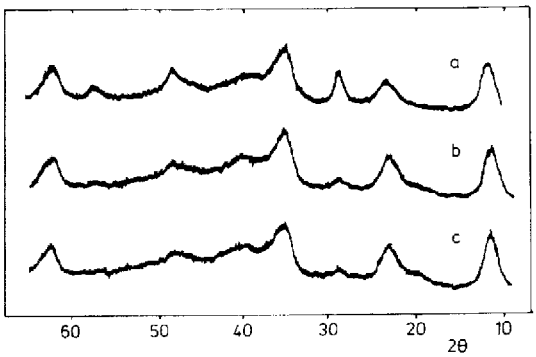

Fig. 2. Effect of drying treatment on the structure as determined by XRD for sample C-3.0 (Cu $K\alpha$ radiation). (a) C-3.0-a, dried at 110°C in air; (b) C-3.0-b, dried at 70°C in nitrogen; (c) C-3.0-c, dried at 70°C in air.

amount of CeO_2 was present after drying at 110°C while much less was present after drying at 70°C. According to the XRD diagrams, it makes no difference whether the drying atmosphere is air or nitrogen.

The amount of Ce^{4+} in these samples was determined by titration with thiosulphate. After drying in nitrogen at 70°C (C-3.0-b), about one third of the cerium present in the sample was in the 4+ state (and thus 2/3 in the 3+ state); after drying at 110°C, about 60% was in the 4+ state and 40% was present as 3+. These results are in accordance with the XRD measurements, the sample with the highest amount of Ce^{4+} showing the most intense diffraction peaks for CeO_2.

Hence, if cerium is present as Ce^{4+}, it then separates from the takovite phase in the form of poorly crystalline CeO_2. Cerium in the 3+ state does not separate in a form which can be detected by powder XRD. It is possible that Ce^{3+} is built into the takovite structure but, due to the small amounts of Ce^{3+} and the poor crystallinity of the takovite phase, no evidence can be given for this.

The sodium contents of the samples were very low: most samples contained less than 0.010 wt.-% sodium. The maximum sodium percentage after the double washing procedure was 0.029 wt.-%.

Calcination

The process occurring during the calcination of the cerium-promoted samples were identical to those for the unpromoted samples [5]. No extra peaks were found in the DTG pattern, in contrast to the case of the lanthanum-promoted samples, for which peaks were found corresponding to the conversion of $La_2O(CO_3)_2 \cdot xH_2O$ into La_2O_3 [1]. The extra phase which is present in the cerium containing samples (CeO_2) is the thermodynamically most stable form under the conditions used and will be therefore not be transformed further.

The calcined phase

According to XRD measurements, the unpromoted calcined samples consist of poorly crystalline NiO with slightly lower lattice parameters than of pure NiO. A similar observation has been reported previously, and it was explained by assuming that the NiO phase contains a small amount of Al_2O_3 [6]. After calcination of the cerium containing samples, CeO_2 was found to be present in most of the samples; only in the samples with the lowest amounts of cerium was no CeO_2 observed using XRD. The degree of crystallinity of the CeO_2 phase remained the same as in the comparable uncalcined samples. The NiO phase in the cerium-promoted samples had slightly lowered lattice parameters compared with pure NiO, in agreement with the results obtained for unpromoted samples. The NiO particle sizes were not influenced by the presence of cerium.

Reduction

The DTG profiles obtained for the reduction process consisted of a single peak for all the samples studied. No differences were found within any series as a function of the amount of cerium present. The samples of the E-series (Ni/Al=9) could be reduced more easily than those of the C and D-series (Ni/Al=2.5 and 3, respectively). This is in agreement with the observation made previously that higher nickel contents give rise to improved reducibility [5].

The reduced phase

After reduction and passivation, the majority of the cerium containing samples contained a separate CeO_2 phase, as was the case before and after calcination. Only in samples with small amounts of cerium (<1 mol-%) was no CeO_2 observed (C+D-series). In the E-series, no CeO_2 phase was present up to 2.7 mol-% cerium; sample E-4.3, however, contained CeO_2. The intensity of the CeO_2 reflections had decreased in comparison to the equivalent uncalcined and calcined samples.

The nickel particle sizes were calculated from X-ray line broadening (XLB) measurements according to the method described in the Experimental section in the previous paper [1]. The results for the samples of series D are given in Table 1. Since the agreement between the particle sizes calculated from the (200) and (111) reflections was good, only those based on the (200) reflections are given. The values were calculated for hemi-spherical particles; if the calculation is carried out assuming spherical particles, slightly different values are found but the trends remain the same [7].

It can be seen that there is little effect of the amount of cerium on the nickel particle sizes; these tend to increase slightly with increasing amounts of cerium. However, the differences are small and it is therefore to be expected that

TABLE 1

Nickel particle sizes, calculated from XLB measurements on the (200) reflection, assuming hemispherical particles for samples of the D-series

Sample	D-0.0	D-0.5	D-1.0	D-2.0	D-4.0	D-5.1	D-6.0	D-8.0
d_v (nm)	10.2	10.5	10.5	10.2	11.0	11.5	11.0	12.0

the samples within this series have nearly identical surface areas. The samples of the C-series (reduced at 600°C) and the E-series (reduced at 400°C) had slightly lower nickel particle sizes than those of the D-series; as with the D-series hardly any influence of the amount of cerium on the particle sizes could be observed for these samples.

Catalytic activity

In this section, the results of the catalytic activity measurements are given, the activity being expressed in mol carbon monoxide converted per gram of nickel per hour at a temperature of 300°C; the apparent activation energies were determined in the range 220–300°C. The results obtained are plotted in Figs. 3 (series D), 4 (series C, dried at 70 or 110°C) and 5 (series E).

As can be seen from Figs. 3–5, the presence of cerium increases both the catalytic activity and the overall (apparent) activation energy. The increase in both is most pronounced at low percentages of cerium. As the amount of cerium is increased further, the activity also continues to increase but less steeply. The effect of the drying temperature on the catalytic activity is shown in Fig. 4. Drying at 70°C instead of at 110°C leads to a higher catalytic activity. It is shown in Fig. 5 that the samples of the E-series have the highest activities of all the samples investigated.

The specific activities (in arbitrary units per m^2 nickel at 300°C) were calculated according to eqn. (3) and are given in Figs. 6 and 7:

$$r(/m^2Ni) = r(/gNi) \cdot d_v \qquad (3)$$

It was assumed that the nickel particle size (d_v) has an inverse relationship with the nickel surface area. The specific activities of the cerium-promoted samples (Figs. 6 and 7) are a factor 2–3.5 larger than those of the unpromoted samples. All of the samples are relatively close to the lines; there is a small effect of the drying temperature on the specific activity (series C). The samples from the E-series have a higher specific activity than those of the two other series.

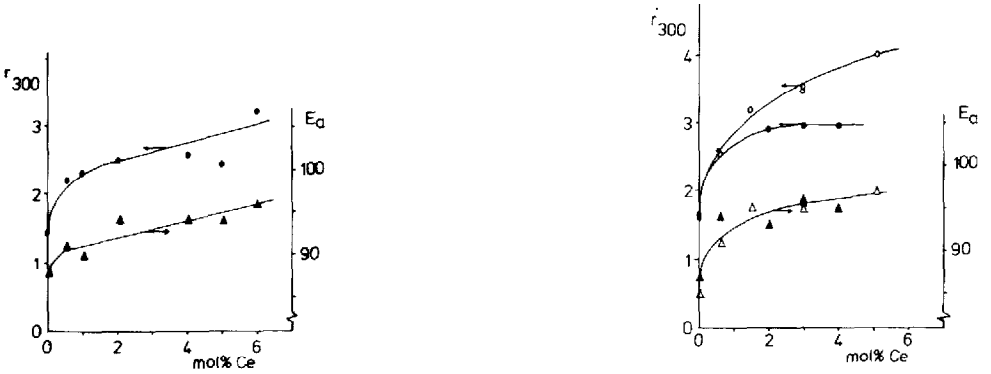

Fig. 3. Catalytic activity (●) [mol carbon monoxide/(gNi·h) at 300°C] and overall (apparent) activation (▲) energies (kJ/mol) for samples of the D-series, all samples dried at 110°C.

Fig. 4. Catalytic activity (●, ○) [mol carbon monoxide/(gNi·h) at 300°C] and overall activation energy (▲, △) (kJ/mol) for samples of the C-series, dried at 70°C (open symbols) or 110°C (closed symbols).

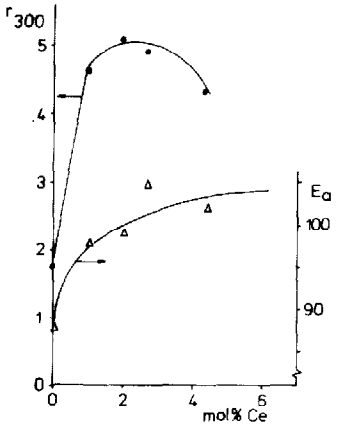

Fig. 5. Catalytic activity (●) [mol carbon monoxide/(gNi·h) at 300°C] and overall activation energy (△) (kJ/mol) for samples of the E-series, dried at 110°C.

Comparison with lanthanum promoted nickel-alumina

The specific activities of the two lanthanum series (A and B) are given in Figs. 6 and 7 for comparison purposes. At small percentages of promoter for a series with Ni/Al $\simeq$ 2.5 (series A, [1]), lanthanum was built into the takovite structure of the precursor. At higher mol percentages phase separation of lanthanum occurred, leading to highly crystalline $La_2O(CO_3)_2 \cdot xH_2O$ (x=1–2). In a lanthanum-promoted series with Ni/Al $\simeq$ 9 (series B, [1]), no phase separation was observed. In the cerium-promoted samples with Ni/Al = 2.5 or 3.0 (series C and D respectively), however, phase separation was observed at very

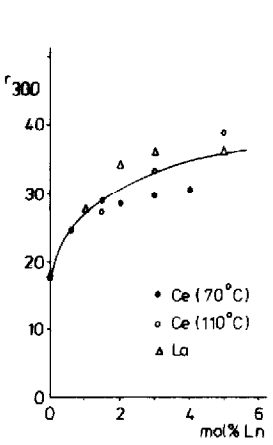

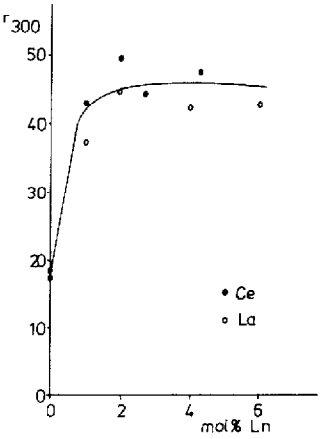

Fig. 6. Specific catalytic activity (a.u. at 300 °C) of cerium and lanthanum promoted samples, Ni/Al ≃ 2.5 (Series C and A [1] resp.), both reduced at 600 °C.

Fig. 7. As Fig. 6, Ni/Al ≃ 9 (series E and B [1] resp.), both reduced at 400 °C.

low percentages of cerium. The new phase was poorly crystalline CeO_2. In a series with Ni/Al = 9.0, phase separation was observed only at the highest amount of cerium (4.3 mol-%).

After calcination and reduction, the nickel particle sizes decreased slightly with increasing amounts of lanthanum (< 5 mol-%). In cerium-promoted samples, however, the particle sizes tended to increase very slightly. The specific activities for both lanthanum- and cerium-promoted samples behaved in a very similar way, and were nearly equal in absolute magnitude, as can be seen from the results of Figs. 6 and 7. The specific activity increased very sharply at low percentages of promoter and became almost constant at higher percentages. The highest specific activities for both promoters were reached in the series with Ni/Al ≃ 9, reduced at 400 °C. The samples of the lanthanum series (with Ni/Al ≃ 9) which were reduced at 600 °C had a somewhat lower specific activity than comparable samples after reduction at 400 °C [1].

This indicates that the temperature of reduction rather than the Ni/Al-ratio causes the difference in specific activity. The activation energies for the methanation of carbon monoxide increased upon addition of the promoter, the increase in the case of lanthanum-promoted samples being somewhat larger than for the cerium-promoted materials.

One of the conclusions of the investigation of lanthanum promotion was that an interaction must occur between the promoter and the nickel in order to explain the observed chemisorption properties and activity patterns. In the investigation reported here, it was shown that samples which contain a relatively small amount of a separate phase of CeO_2 have a higher specific activity than samples with identical overall composition but with a higher amount of

the separate phase of CeO_2 (see Fig. 2). This again indicates that some sort of interaction has to occur between cerium and nickel and that this interaction is stronger whenever the promoter has a smaller degree of crystallinity. This interaction may arise at the interface between CeO_x crystallites on top of nickel crystallites and the crystallites themselves or at the borderline of the nickel crystallites. Since both the lanthanum- and cerium-promoted samples behave very similarly in the carbon monoxide methanation reaction, it seems that the cause of the enhancing effect of both promoters is also the same.

CONCLUSIONS

Cerium enhances the activity of nickel–alumina coprecipitated catalysts in the carbon monoxide methanation reaction. The enhancement is accompanied by an increased apparent activation energy. Part of the cerium present in most of the passivated promoted samples exists as poorly crystalline CeO_2. The amount of this phase which separates is partly determined by the drying procedure used after precipitation and washing. Although cerium and lanthanum behave differently in determining the catalyst structure, their behaviour in the carbon monoxide methanation reaction is very similar and the specific activities of both types of material are nearly equal.

ACKNOWLEDGEMENTS

We would like to thank Richard Smits and Peter van der Woude for preparing some of the samples, Jaap Boeijsma for his help with XRD measurements and Wim Lengton and Hans Weber for performing the chemical analyses.

REFERENCES

1 H.G.J. Lansink Rotgerink, R.P.A.M. Paalman, J.G. van Ommen and J.R.H. Ross, Appl. Catal., 45 (1988) 257.
2 M.R. Gelsthorpe, K.B. Mok and J.R.H. Ross, J. Mol. Catal., 25 (1984) 253.
3 A.R. Stokes and A.J.C. Wilson, Proc. Cambridge Philos. Soc., 38 (1942) 313.
4 E.C. Kruissink, L.L. van Reijen and J.R.H. Ross, J. Chem. Soc., Faraday Trans. 1, 77 (1981) 649.
5 H.G.J. Lansink Rotgerink, H. Bosch, J.G. van Ommen and J.R.H. Ross, Appl. Catal., 27 (1986) 41.
6 E.B.M. Doesburg, P.H.M. de Korte, H. Schaper and L.L. van Reijen, Appl. Catal., 11 (1984) 155.
7 H.G.J. Lansink Rotgerink, Thesis, University of Twente, 1988, Ch. 4.